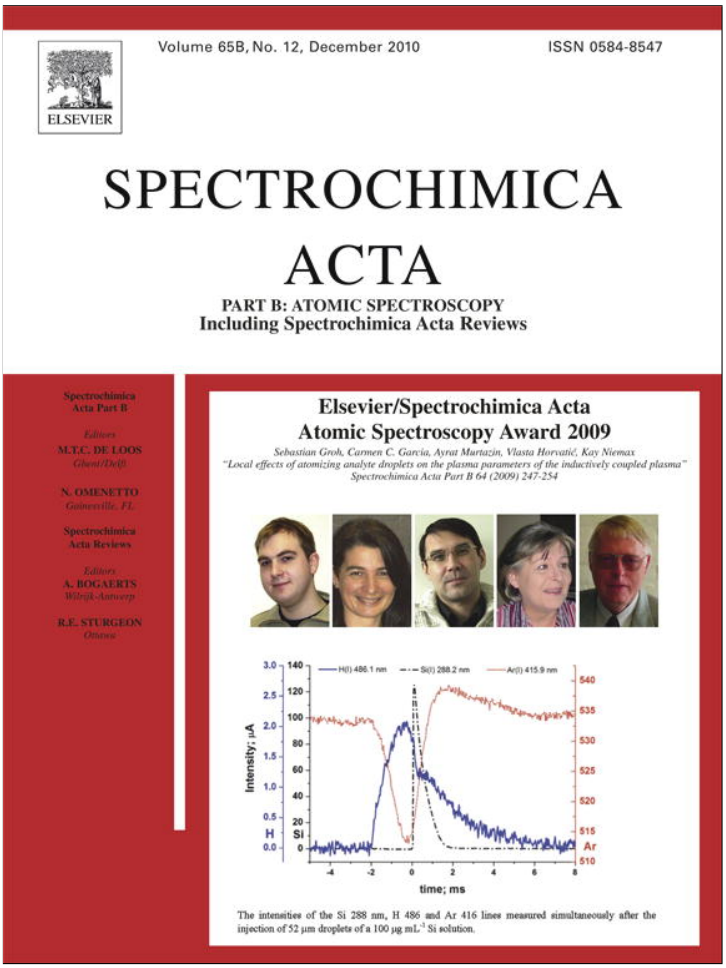

Spectrochimica Acta Part B 65 (2010) 1029–1032

Contents lists available at ScienceDirect

Spectrochimica Acta Part B

journal homepage: www.elsevier.com/locate/sab

Spatially resolved emission using a geometry-dependent system function and its application to excitation temperature profile measurement

Hoyong Park [a], Wonho Choe [a,*], S.J. Yoo [b]

[a] Department of Physics, Korea Advanced Institute of Science and Technology, 335 Gwahangno, Yuseong-gu, Daejeon 305-701, Republic of Korea
[b] National Fusion Research Institute, 113 Gwahangno, Yuseong-gu, Daejeon 305-333, Republic of Korea

ARTICLE INFO

Article history:
Received 30 March 2010
Accepted 11 November 2010
Available online 23 November 2010

Keywords:
Line of sight
Reconstruction
System function
Excitation temperature

ABSTRACT

As typical emission spectroscopy involves chord integration along the line of sight, a local measurement with high spatial resolution is attempted using simple lens optics in this work. In the experiment, chord integrated optical plasma emission profile was measured by moving a scanning lens located outside the plasma. The measured emission intensities were spatially reconstructed by employing a geometry-dependent system function, and the local (i.e., only from the lens focal point) emission intensities were obtained with all out-focused emissions subtracted. The 34 different Ar I emission lines spatially reconstructed in this way were used to determine excitation temperature (T_{exc}) of the argon plasma by the Boltzmann plot method. Being different from the plasma driven at 13.56 MHz where a rather uniform profile was obtained, the spatial profile of T_{exc} from the plasma driven at 90 MHz showed a hollow profile, which is similar to that of the electron temperature (T_e) measured by a Langmuir probe. This hollow profile is attributed from the electromagnetic phenomena such as skin effect and standing wave effect. The similar spatial tendency of T_{exc} and T_e implies that T_{exc} can be a representative of T_e. This is particularly useful for the cases in which conventional Langmuir probe measurements are limited, such as in large size plasmas.

1. Introduction

Large area capacitive discharges driven at frequencies higher than the conventional 13.56 MHz have recently attracted much attention in both plasma physics and in the semiconductor and display industries as processing plasma sources [1–4]. Large size plasma sources are required in such areas for the large size panel fabrication of LCDs and photovoltaic solar cells (for instance, the glass substrate size for the 8th generation LCD panel is such as 2200 mm × 2500 mm, and the size of the processing plasma is larger than that). At large plasma sources where the plasma dimension becomes comparable to the wavelength of the driving radio frequency (rf), physical phenomena such as standing wave and skin effects are found to occur, which do not take place at lower driving frequencies [5]. These electromagnetic phenomena tend to diminish the degree of plasma uniformity [2,5,6]. At large size, therefore, achieving high spatial uniformity of the plasma and measuring this with high accuracy have become important research issues [7–9]. As one of the most prevalent and versatile means of measuring spatial uniformity, optical emission spectroscopy (OES) is a useful diagnostic tool, but it inevitably involves chord-integrated measurements along the line of sight. Hence, either inversion or tomographic reconstruction is required to obtain spatially-resolved local information inside the plasma [10].

In this paper, we introduce the technique that enables to measure the spatial profile from the chord-integrated optical emission from the plasma using only simple lens optics. It was found that with the spatially-resolved excitation temperature compared with the electron temperature obtained by a rf compensated Langmuir probe, the electromagnetic phenomena were observed at the 90 MHz driving frequency.

2. Experimental

A schematic diagram of the experimental setup for visible emission measurement is presented in Fig. 1. The argon plasma generated in a rectangular chamber is a typical capacitively coupled type with the rectangular electrode size of 300 mm × 200 mm. The distance between the top and the bottom electrodes was fixed at 40 mm, so that the vertical (or z-directional) plasma size L_z is 40 mm. The top electrode was powered by a rf generator at either 13.56 MHz or 90 MHz at 300 W, while the bottom one was grounded. The collection optics consists of two circular lenses (CVI, AAP-500.0-50.8) made of BK7 and SF2 of 500 mm focal length and 50.8 mm diameter in order to collect the plasma emission. Both lenses had achromatic coating to avoid the chromatic aberration in obtaining wavelengths from 415 nm to 810 nm. The two lenses were placed on a linear rail to scan the emission light, and the whole collection optics was contained

* Corresponding author.
E-mail address: wchoe@kaist.ac.kr (W. Choe).

0584-8547/$ – see front matter © 2010 Elsevier B.V. All rights reserved.
doi:10.1016/j.sab.2010.11.008

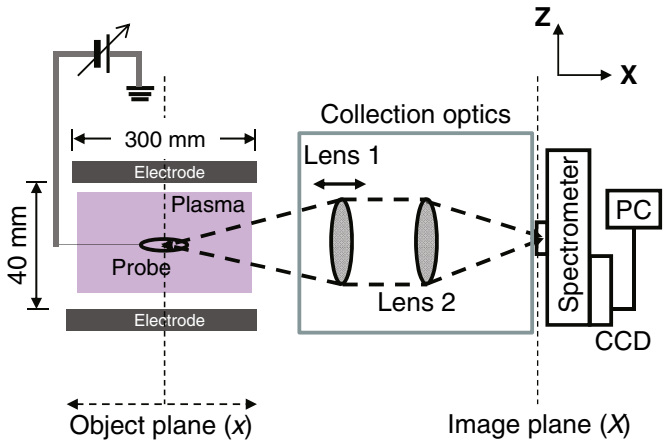

Fig. 1. Schematic of the experimental setup (side view, not in scale). The capacitive plasma was produced between the rectangular top and bottom electrodes (300 mm × 200 mm) with the gap distance of 40 mm. The plasma emission was measured in the X direction by moving Lens 1, while Lens 2 was used to focus the emission to the entrance slit of the spectrometer. A Langmuir probe was inserted inside the plasma to obtain electron temperature profile, i.e., $T_e(x)$.

in a black metal housing of 1 m length to block the unnecessary stray light. The emission profile was scanned by Lens 1, of which travel length was as large as 500 mm. The long scanning length of the collection optics was demanded in order to scan the large size plasma. A spectrometer (CHROMEX 250is) and a charge-coupled device (CCD) detector (SBIG, ST-9XE) were used to obtain the argon atomic line intensities. The entrance slit size of spectrometer was set at 0.05 mm (width) × 20 mm (height), and a pin-hole of 1 mm in diameter was placed in front of the entrance slit. The excitation temperature was measured by the Boltzmann plot method using the relative line intensity ratio of Ar I emission lines [11], while the electron temperature and density were measured by a commercial Langmuir probe (PLASMART, SLP2000).

3. Results and discussion

3.1. Reconstruction procedure: preliminary tests of the system function

In the case of chord-integrated collection of the emission, the emission detection only at the lens focal point is essential for measuring the spatial profile of the emission with high accuracy. In this study, an improvement of spatial profile measurement is made by employing a technique of eliminating the out-focused emission by applying a geometry-dependent system function to the measured chord-integrated plasma emission data. The system function was obtained in advance from a simple optics setup consisting of two achromatic lenses, a mercury lamp, and a spectrometer.

The purpose of the system function is to find a local intensity profile $f(x)$, which is the intensity profile only at the lens focal points, out of the measured chord-integrated intensity profile $g(X)$, which is the profile contributed both from the lens-focused intensities and the out-focused intensities, from a large size emission source. The measured intensity $g(X)$ can be expressed as convolution of two functions, $f(x)$ and $h(X-x)$:

$$g(X) = \int_{-\infty}^{\infty} f(x)h(X-x)dx \ , \tag{1}$$

where X and x are the position domains in the image and object planes, respectively, and $h(X-x)$ is a geometry-dependent system function determined based on the optical setup. In Eq. (1), $g(X)$ can be converted into the multiplication of the two functions of $F(\kappa)$ and $H(\kappa)$ by the convolution theorem of the Fourier transform,

$$G(\kappa) = F(\kappa) \otimes H(\kappa), \tag{2}$$

where κ is the wave number, and $G(\kappa)$, $F(\kappa)$, $H(\kappa)$ are the Fourier transformed functions of $g(X)$, $f(x)$, $h(X-x)$, respectively. Consequently, $F(\kappa)$ can be obtained from Eq. (2), and $f(x)$ is finally obtained from the inverse Fourier transform of $F(\kappa)$ as follows:

$$f(x) = \frac{1}{\sqrt{2\pi}} \int_{-\infty}^{\infty} F(\kappa) e^{-i\kappa x} d\kappa. \tag{3}$$

The procedure for obtaining the local intensity profile $f(x)$ mentioned above is defined as "reconstruction" in this paper. Since $f(x)$ is obtained from the chord-integrated intensity $g(X)$ using the system function $h(X-x)$, it is important to define $h(X-x)$ prior to the reconstruction.

In order to experimentally determine $h(X-x)$, we used a combination of a mercury lamp (ACTON, MS416) and an aperture of 1 mm diameter that was small enough to be considered as a point source (i.e., the light source much smaller than the sight line or the plasma dimension). The diameter and its focal length of the collection lens were 50 mm and 500 mm, respectively. The measured intensity by moving the lamp and aperture combination along the lens axis is presented as circles in Fig. 2a, and we used this profile as $h(X-x)$. As expected, the largest intensity is shown at the lens focal point (0 mm position in the figure) and the out-focused emission intensities quickly drop from the lens focal point. This result can be explained by both the projected solid angle of the point source emission and the broadened image area of the point source on the entrance slit. The measured intensity profile shown in Fig. 2a is also known as the system étendue function [12]. It is noted that the system function h shown in Fig. 2a is the arithmetic average of the intensities of 476 nm, 696 nm, and 810 nm Hg lines.

The reconstructed intensity profile $f(x)$ by letting $g = h$ showed a delta-function type as expected. On the other hand, the dashed (−) curve shown in Fig. 2a indicates $f(x)$ reconstructed with letting $g(X)$ be the 810 nm intensity. Other 476 nm and 696 nm lines showed the similar $f(x)$ profile. As depicted in an inset of Fig. 2a, the profile $f(x)$ has full width at half maximum (FWHM) of about 12 mm with base width of about 20 mm. This could be attributed to the followings: firstly, finite focal spot size (showing the uniform lamp intensity in the direction normal to the lens axis around the lens focal point, which was about 10 mm under our experimental setup). Secondly, the finite size of the light source (extension of the Hg lamp in the x direction being about 5 mm). Thirdly, generally good but imperfect achromatic condition of our collection optics system. Anyhow, the out-focused emissions are eliminated considerably by the reconstruction, showing the intense lamp emission only near the focal point of the lens. It is also worth noting that the fact that the resolution of reconstructed intensity profile is about 12 mm is probably the best-case scenario because the source is a point source and there is no other emission from other locations along the line-of-sight (x-axis) integration, i.e., a very clean background.

The system function h discussed here is 'one-dimensional' since it was obtained as the lamp (point source) was moved along the lens axis. However, it should be 'three-dimensional' for large emission sources such as volumetric plasmas because the emission reaches the collection optics in the three-dimensional way (both up-down and left–right), as illustrated in Fig. 2b. To account for this, Eq. (1) is extended as

$$\begin{aligned} g(X) &= \iiint f(x)f(y)f(z) \cdot h(X-x, Y-y, Z-z)dxdydz \\ &= \int_{-\infty}^{\infty} f(x)\left[\int_{y(x)}^{y(x)} f(y) \cdot \int_{-z(x)}^{z(x)} f(z) \cdot h(X-x, Y-y, Z-z)dydz\right]dx \\ &\equiv \int_{-\infty}^{\infty} f(x)h^*(X-x)dx, \end{aligned} \tag{4}$$

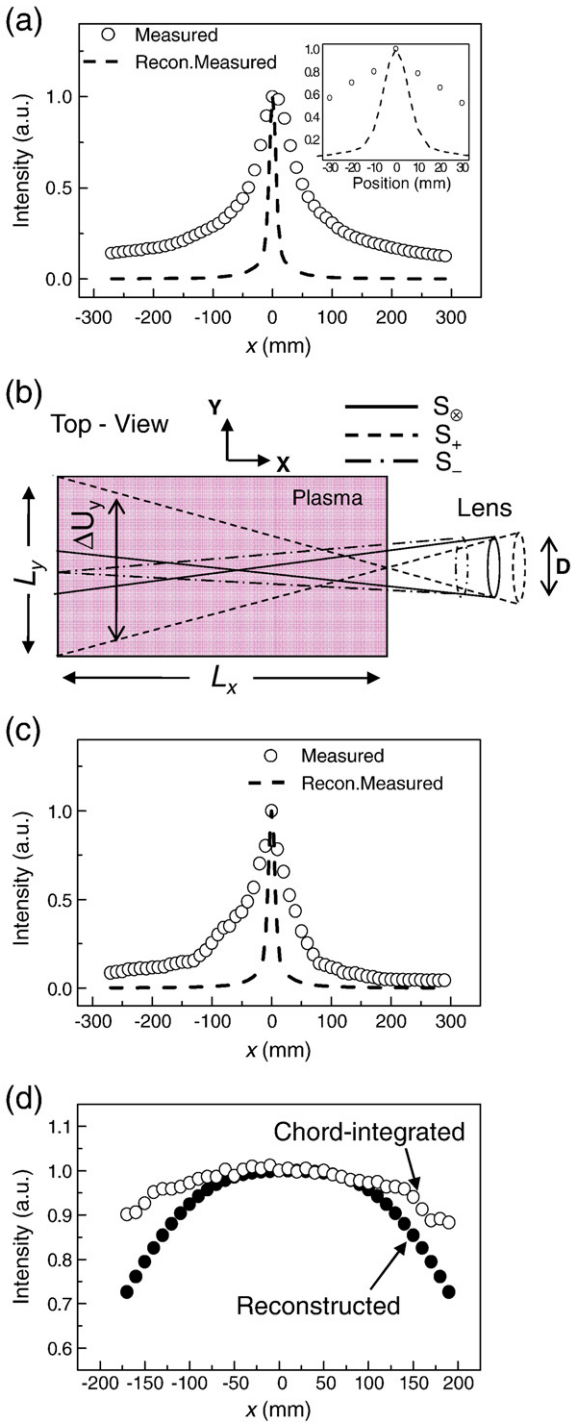

Fig. 2. (a) Measurement of the system function. The circles represent the measured intensity profile using a point source consisting of a mercury lamp and an aperture. The reconstructed intensity profile using the measured system function is plotted as dashed (---) curve. The reconstructed profile in an expanded scale is depicted as an inset. (b) The measurement span of plasma emission through the lens when the lens is focused on the plasma center and edges in top-view, respectively. (c) Measurement of the modified system function. The reconstructed intensity profile is plotted as dashed (---) curve. (d) The measured intensity profile of 516 nm of Ar I emission (open symbols) and its reconstructed intensity profile (closed symbols) as a function of lens focal point.

where Y, Z, y, and z are the position domains in the image (Y,Z) and the object (y,z) planes, respectively. In Eq. (4), $h^*(X-x)$ is the modified system function (MSF).

In Fig. 2b, the boundaries of measurement span through the collection lens are represented as $S_{\otimes}$, S_+ and S_-. Here, $S_{\otimes}$ indicates the measurement span when the lens is focused on the plasma center, whereas S_+ and S_- represent those when focused on the plasma edges. As shown in Fig. 2b, the Y-directional finite length of uniform intensity ΔU_y should be considered in reconstruction because the detecting size of the plasma through the lens (in the case of S_+) becomes comparable to the Y-directional plasma size L_y. On the other hand, the Z-directional component is ignored because the measurement span through the lens along the Z-direction (e.g. electrode gap of 40 mm) is much smaller than the lens focal length (e.g. 500 mm in this experiment). Furthermore, since the MSF includes the Y-directional plasma emission $f(y)$, the half of the plasma is assumed to give uniform emission intensity along the Y-direction, i.e., $f(y)=1$. In addition, we measured ΔU_y of the lamp intensity by moving the light source in the y-direction at fixed x and then the same procedure was repeated at different x positions, i.e., by a full 2-dimensional scan of the light source in both x and y direction. It was found that the system function $h(X-x,Y-y)$ remained the same, irrespective of ΔU_y, or $h(X-x, Y-y)$ is constant at least within the measured ΔU_y.

Therefore, the MSF in Eq. (4) becomes

$$h^*(X-x) = \int_{-y(x)}^{y(x)} f(y)\cdot h(X-x)dy, \qquad (5)$$
$$= h(X-x)\cdot \Delta U_y.$$

With the three-dimensional effects in Eq. (5), the measured intensity profile $h^*(X-x)$ is presented as circles and the reconstructed intensity profile is shown as the dashed (—) curve in Fig. 2c. Fig. 2d shows the measured intensity profile of 516 nm of Ar I emission (open symbols) from the plasma and its reconstructed intensity profile (closed symbols) using MSF given in Eq. (5). Using this technique, the spatially resolved excitation temperature of the Ar emission from the plasma was obtained.

3.2. Application of the reconstructed intensity profile to the plasmas

Fig. 3a and b represent the horizontal profiles (along the lens axis) of the excitation temperature T_{exc} and the electron temperature T_e, respectively, obtained from a 300 mm × 200 mm sized plasma driven at very high frequency (VHF) of 90 MHz. The excitation temperature was determined by the Boltzmann plot method [11] using the measured 34 different Ar I emission lines. Each open circle in Fig. 3a (for instance, at a certain x) was obtained based on the line-integrated intensity $g(X)$ with the lens focal point located at that particular position x. In other words, the measured 34 Ar I lines were simply used for the Boltzmann method to get $T_{exc}(x)$. On the other hand, the closed circles in Fig. 3a were obtained based on the reconstructed intensities $f(x)$, i.e., 34 Ar I lines at x were all reconstructed first, and then they were used in the Boltzmann method.

A few findings are made from the result. First of all, a large discrepancy is seen between the T_{exc} profile based on the line-integrated intensity (open symbol) and that based on the reconstructed intensity (closed symbol) (Fig. 3a), in which the reconstructed one shows the more hollow profile. The model accounting for the substantial skin depth or standing wave effects is reported at frequency higher than 70 MHz [2], and the electrode edge asymmetry in rf plasma increases localized electric field at the edge of the electrodes. Therefore, the plasma becomes more intense near the edges [13]. The inductive electric field near the electrode edge also creates strong plasma non-uniformity at high frequency [14]. The increasing trend of both T_e and T_{exc} toward the electrode edge shown in Fig. 3a and b is believed to be attributed from these physical effects.

Second, the fact that T_{exc} is about three times lower than T_e as inferred from Fig. 3a and b and also the electron density in our experiment (~10^{10} cm^{-3}) is lower than the critical density given by the Griem criterion [15] indicates that this plasma is in non-equilibrium.

Third, the reconstructed spatial profile of T_{exc} has the similar tendency with that of T_e. It is understandable because $T_{exc} \propto I_1(\mathrm{Ar})/I_2$

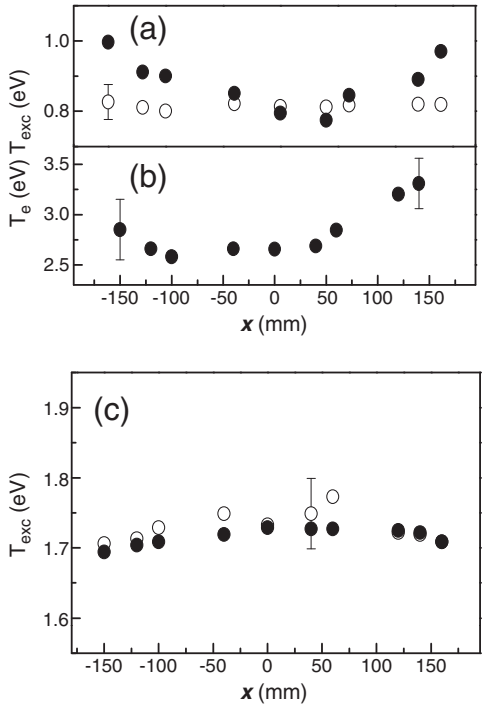

Fig. 3. (a) The spatial profile of (a) the excitation temperature without (open symbol) and with (closed symbol) the reconstruction, and (b) the electron temperature by a Langmuir probe. The operating condition was Ar 300 mTorr and 300 W at 90 MHz. (c) The excitation temperature profile without (open symbol) and with (closed symbol) the reconstruction at Ar 300 mTorr and 300 W at 13.56 MHz.

$(\mathrm{Ar}) \propto R_{12}(T_e)$, i.e., the spectral line ratio (R_{12}) corresponds to T_{exc} and is related to T_e due to its impact excitation on argon atoms [16]. This result implies that T_{exc} can be a representative of T_e in non-equilibrium plasmas such as the plasma under this experiment. This is particularly useful for the cases in which conventional Langmuir probe measurements are limited, such as in large size plasmas.

Fourth, Fig. 3c depicts T_{exc} profile of the plasma driven at 13.56 MHz in the direction of lens axis without (open symbol) and with (closed symbol) reconstruction, respectively. At conventional 13.56 MHz rf frequency, T_{exc} profiles are not considerably different with and without the reconstruction, and they also showed the similar tendency with the T_e profile. Therefore, by comparing the reconstructed and the line-integrated profiles, the reconstruction result in Fig. 3a implies the spatially non-uniform T_e, such as the hollow shaped profile shown in Fig. 3b at 90 MHz, as opposed to the spatially uniform electron temperature at 13.56 MHz.

4. Conclusion

We developed an accurate OES measurement technique for the spatial emission profile by eliminating the out-focused plasma emission. This was accomplished by the simple lens optics and reconstruction process using the geometry-dependent system function. Experiments performed at 90 MHz driving frequency with this technique show the hollow-shaped spatially resolved excitation temperature profile (higher T_{exc} near the edge), which is attributed from the electromagnetic phenomena. This profile is consistent with the electron temperature measured by a Langmuir probe. It is also confirmed at 13.56 MHz that both profiles of T_e and T_{exc} are consistent. This may be particularly useful for the cases in which conventional Langmuir probe measurements are limited, such as in large size plasmas.

Acknowledgements

This work was supported by the National R&D Program through the National Research Foundation of Korea (NRF) funded by the Ministry of Education, Science and Technology (2010-0020037). The authors would like to thank Drs. C. R. Seon and S. K. Ahn for their valuable discussions and experimental helps.

References

[1] D. Leongardt, S.G. Walton, D.D. Blackwell, W.E. Amatucci, D.P. Murphy, R.F. Fernsler, R.A. Meger, Plasma diagnostics in large area plasma processing system, J. Vac. Sci. Technol. A 19 (2001) 1367–1373.
[2] M.A. Lieberman, J.P. Booth, P. Chabert, J.M. Rax, M.M. Turner, Standing wave and skin effects in large-area, high-frequency capacitive discharges, Plasma Sources Sci. Technol. 11 (2002) 283–293.
[3] P. Chabert, J.L. Raimbault, J.M. Rax, M.A. Lieberman, Self-consistent nonlinear transmission line model of standing wave effects in a capacitive discharge, Phys. Plasma 11 (2004) 1775–1785.
[4] H.H. Goto, H.D. Lowe, T. Ohmi, Independent control of ion density and ion bombardment energy in a dual RF excitation plasma, IEEE Trans. Semicond. Manuf. 6 (1993) 58–64.
[5] A. Perret, P. Chabert, J.P. Booth, J. Jolly, G. Guillon, Ph. Auvray, Ion flux nonuniformities in large-area high-frequency capacitive discharges, Appl. Phys. Lett. 83 (2003) 243–245.
[6] I. Lee, D.B. Graves, M.A. Lieberman, Modeling electromagnetic effects in capacitive discharges, Plasma Sources Sci. Technol. 17 (2008) 015018.
[7] Y. Wu, M.A. Lieberman, The influence of antenna configuration and standing wave effects on density profile in a large-area inductive plasma source, Plasma Sources Sci. Technol. 9 (2000) 210–218.
[8] H. Schmidt, L. Sansonnens, A.A. Howling, Ch. Hollenstein, M. Elyaakoubi, J.P.M. Schmitt, Improving plasma uniformity using lens-shaped electrodes in a large area very high frequency reactor, J. Appl. Phys. 95 (2004) 4559–4564.
[9] T. Meziani, P. Colpo, F. Rossi, Design of a magnetic-pole enhanced inductively coupled plasma source, Plasma Sources Sci. Technol. 10 (2001) 276–283.
[10] Y. Miyoshi, Z.L. Petrovic, T. Makabe, Optical computerized tomography of the E–H transition in inductively coupled plasmas in Ar and Ar–CF_4 mixtures, J. Phys. D 35 (2002) 454–461.
[11] S.Y. Moon, W. Choe, H.S. Uhm, Y.S. Hwang, J.J. Choi, Characteristics of an atmospheric microwave-induced plasma generated in ambient air by an argon discharge excited in an open-ended dielectric discharge tube, Phys. Plasma 9 (2002) 4045–4051.
[12] F. Fournier, J. Rolland, Design methodology for high brightness projectors, J. Display Technol. 4 (2008) 86–91.
[13] A.A. Howling, L. Sansonnens, J. Ballutaud, Ch. Hollenstein, J.P.M. Schmitt, Nonuniform radio-frequency plasma potential due to edge asymmetry in large-area radio-frequency reactors, J. Appl. Phys. 96 (2004) 5429–5440.
[14] S.K. Ahn, H.Y. Chang, Experimental observation of the inductive electric field and related plasma nonuniformity in high frequency capacitive discharge, Appl. Phys. Lett. 93 (2008) 031506.
[15] H. Griem, Validity of Local Thermal Equilibrium in Plasma Spectroscopy, Phys. Rev. 131 (1963) 1170–1176.
[16] R.F. Boivin, J.L. Kline, E.E. Scime, Electron temperature measurement by a helium line intensity ratio method in helicon plasmas, Phys. Plasmas 8 (2001) 5303–5314.